

Calibration of Traffic Incident Simulation Models Using Field Data

Samuel Y. R. Rompis^{1,2*}, Filmon G. Habtemichael³

¹Department of Civil Engineering, Sam Ratulangi University, Indonesia

²National Center for Sustainable Transportation Technology, Indonesia

³Battelle Memorial Institute, Columbus, OH, USA

*Email: semrompis@fulbrightmail.org, semrompis@unsrat.ac.id

Abstract

This study presents a methodology to calibrate a traffic incident simulation model, particularly in a freeway. The queue length was used as the objective of the simulation model calibration in this study. The simulation model was set up using Traffic Simulation Model PTV. VISSIM. Multiple incident durations were simulated, and the generated queue lengths were compared to the observed queue lengths. The observed queue lengths were estimated using the LWR model and shockwave speeds calculated using the field data. The results confirm that calibrated VISSIM incident model can signify the shockwave propagation speeds and queue length in the event of freeway incident. Such a model can be implemented as an instrument for setting up traffic management strategies to alleviate the incident's impact.

Keywords

Calibration; Incidents; LWR; Shockwave; VISSIM

1 Introduction

Incidents are random events that happen anytime and anywhere on freeways with negative impacts on the flow of traffic. Such events obstruct a shoulder, a lane or multiple lanes and may involve vehicle accident, disabled vehicle and spilled load resulting in decreased throughput and increased delay. The Highway Capacity Manual indicated that incidents are the main reason for more than half of congestion and delays [1]. Looking at the incident's impact on freeway operations and taking into account the delay they are in charge of, they deserve in-depth study.

Understanding the impact of incidents is essential to maximize freeway service and minimize their negative effects. The traffic flow theory has been utilized to develop Shock Wave (SW) profiles because of incidents. These profiles are the key tools for attaining the essential variables such as queue length, delay, and the duration of queue dissemination. An example of this is that if the time required for dissolving the queue could be accurately estimated, reliable information regarding traffic conditions could be disseminated to road users. Thus, it leads to an effective traffic management strategy that makes the transportation system efficient, greener, and even safer.

A microscopic traffic simulation model has become very popular in the discipline of traffic engineering, transportation system design as well as traffic operations and management. This model delivers an

accommodating environment for measuring different traffic management strategies, e.g., minimizing incident-induced delay and emissions as well as designing optimal incident response management schemes. A researcher has employed traffic simulation models for improving mobility and making transportation systems more efficient [2]–[4]. However, the application of simulation to analyze incidents and their impact has been somewhat limited.

The ability to correctly simulate incidents in microscopic simulation models is the first step in analyzing the impact of freeway incidents and taking appropriate actions to address the problem. However, it appears that there is an absence of a satisfactory technique for appropriately simulating traffic incident in the simulation model. To successfully mimic the impact in microscopic traffic simulation models requires the model's parameters to be accurately calibrated using valid objective measurement resulted from the incident. This paper is focused on calibrating microscopic traffic simulation models to model the impacts of incidents.

It is desirable to calibrate microsimulation models such that queue lengths caused by incidents reflect the real-world conditions. However, it is problematic to measure the queue lengths in the field directly, due to the variation in travel demand, presence, and absence of on-off ramps and weaving sections. Therefore, in this research, the simulation model is calibrated so that the resulting SW speeds from the model reflects the ones

that observed in the field. To achieve this, the queue lengths from the simulation model were compared to those predicted from the LWR, where the LWR model parameters are predicated on the field-observed SW speeds.

The LWR model is a kinematic wave theory introduced by Lighthill, Whitham [5], and Richards [6] which is a well-known method of structuring SW profiles and estimating queue lengths. To obtain queue length from the LWR model, accurate SW speeds as an input to the LWR model would be required. Conventionally, the Fundamental Diagram (FD) has been employed as a base to estimate the SW speeds. Even though LWR model has proven to be reliable and authentic means of representing SW profiles and approximating queue lengths, its performance can be prominently affected by the uncertainty of the FD from which the SW speeds are obtained. In a study that focused on the analysis of LWR model under uncertain FD, Li et al. [7] concluded that “...if FD cannot be undoubtedly specified, the LWR model will deteriorate and only make reasonable predictions...” A detailed discussion of the impact of uncertainties of FD on the LWR model is discussed in Section 2.2.

Considering the drawbacks of the FD, this paper attempts to utilize SW speeds observed from the field to develop LWR-based SW profiles and queue lengths. Given two traffic sensors placed at upstream and downstream locations on a homogenous freeway segment without on-off ramps, SW speeds can be easily estimated from the field. This way, the shortcomings of using SW speeds estimated from uncertain FD can be overcome.

The purpose of this study is to construct a robust methodology for calibrating incident simulation model by employing field observed SW profiles. A road segment of The Hampton Roads Bridge-Tunnel (HRBT), linking the cities of Norfolk and Hampton, Virginia, was utilized as a site to estimate the SW speed from the field.

This paper is arranged in the following manner. After this introductory section, a review of the literature on LWR and uncertainties of FD is provided. The next part is a discussion on the methodological approach of this study. Description of the experiment conducted is presented, the findings were validated, and at last, conclusions were drawn.

2 Literature Review

2.1 LWR macroscopic model

Lighthill, Whitham [5], and Richards [6] introduced the first dynamic traffic model which employed the FD and the traffic conservation law. The equation of fluid dynamics continuity became the base of this traffic flow model and is recognized as the first order of LWR traffic flow model. The LWR model is discussed in detail in Section 3.3.

Researchers have conducted traffic SW analysis both at macroscopic and microscopic levels in the past. At the macroscopic level, the LWR kinematic SW theory was used to study the dynamics of traffic flow [8] and to develop traffic SW profile on congested urban arterials [9]. Lu and Skabardonis [10] developed a numerical algorithm to assess the SW speed on interstate using vehicle trajectory data. Additionally, the LWR model has been effectively implemented in measuring the incident-induced delay [11], examining the traffic transformation and maximum queue lengths due to incident [12] and estimating the effect to the time and space on freeways [13]. All these studies have exhibited that the LWR model has been recognized as an important instrument in many traffic engineering applications. However, the accuracy of SW profiles and queue lengths estimated using the LWR model heavily depends on the reliability of the FD used to derive the SW speed.

2.2 Uncertainty in FD

FD is the basics of traffic engineering; however, it has been a topic of study for many researchers over the past 80 years [14]. Since the pioneering works of Greenshields [15], which assumed a linear relationship between speed and traffic density, more advanced and complicated models had been proposed, each with its merits and demerits [16]. Though FD has been successfully applied in many applications, several questions have been asked on its performance. The widely scattered flow-density and volume-density relationships, especially around congested traffic conditions, have been identified as the essential concern of FD's dependability [17]. Kerner [18] criticized FD as it fails to reproduce the spatial-temporal features of congestion on freeways, accurately. Given the wide varieties of physical phenomena exhibited by freeway traffic, there is no such thing as a perfect FD which is representative of all traffic conditions. Another concern is the issue of uncertainties in the assumptions that FD makes, its model parameters, and mechanism of data collection to formulate the speed-volume-density relationships. The majority of the researchers worked with density, while the empirical data available for their

study was occupancy. Thus, transforming one parameter into another undermines the accuracy of FD in representing the traffic [19]. Furthermore, model equations derived for fitting curves using the transformed variables are later changed back to the original variables, which can lead to biased results. In multi-regime FDs, the problem of continuity at the boundary of regimes is also another issue that needs to be addressed.

2.3 Microscopic simulation model calibration

Researchers have broadly utilized microscopic simulation models in the field of traffic engineering as a great tool to solve transportation problems. However, the reliability of this model depends so much on how well the parameters were calibrated based on real-life situations. Many studies have been conducted on calibrating the microscopic simulation model, such as in [2]–[4], other studies suggested the model calibration methodology [20]–[22] but very few discussed calibrations of the model in traffic states during incident-induced congestion.

3 Methodology

3.1 Description of study area and data used

The westbound direction of the HRBT corridor, which is a two-lane freeway, linking the cities of Norfolk and Hampton, Virginia, was employed as the study area. The geometric layout of the area is shown in Figure 1. Traffic data (speed, volume, and occupancy) corresponding to the passage collected by three fixed-point sensors were used in this study. The traffic data were aggregated at two-minute intervals. A record of historical incident data, which happened on the segments between detectors No. 1 and 2, was provided by the VDOT. In the freeway section between detectors No. 1 and 3, there are no on-off ramps, and thus vehicle count is conserved.

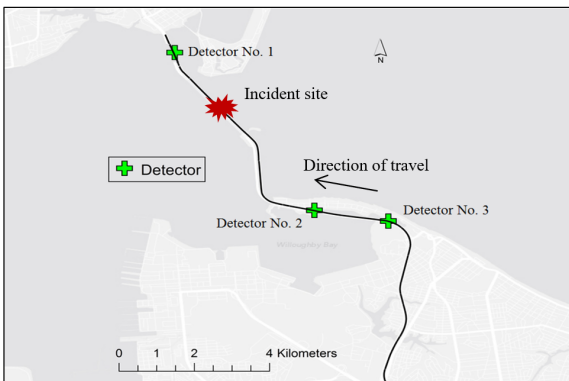


Figure 1 Study area and location of detectors

3.2 Estimating field observed queuing and discharge SW speeds

To determine the queue length, the queuing and the discharge SW speeds are required as inputs to the LWR model (as is discussed in Section 3.3). To estimate the queuing and the discharge SW speeds, time of incident events were matched with the traffic data. This research mainly focuses on SW speeds resulting from incidents blocking both lanes of the WB HRBT corridor. However, the incident data that VDOT provided did not include the number of lanes closed. Therefore, to pick incidents which blocked both lanes, we looked at the volume count provided by detector No. 1. Whenever the volume and speed around the time an incident happened are zero, then we are sure that the incident blocked both lanes.

SWs typically occur at the boundary between two traffic states, e.g., when the speed drops below the speed-at-capacity. In this study, the SW speeds were defined when the speed of traffic drops below 5 kph (3.1 mph) and is sustained until the speed of traffic is more than 10 kph (6.2 mph).

To obtain field-observed queuing and discharge SW speeds, the time when the speed of traffic at detectors No. 2 and 3 dropped were carefully recorded. Also, when a drop-in speed was observed, occupancy should be relatively higher so that we are sure that the slowdown of traffic is because of SW. Since the distance between detectors No. 2 and 3 is fixed (1.61 km or 1 mile), the SW speed will be this distance divided by the difference in time when the speed dropped at detector No. 3 and the time speed dropped at detector No. 2. This is shown in Equations (1) and (2).

$$w_q = \frac{D}{\left(\frac{t_a}{60}\right)} \quad (1)$$

$$w_{ds} = \frac{D}{\left(\frac{t_d}{60}\right)} \quad (2)$$

Where w_q (kph) is the queuing SW speed, w_{ds} (kph) is the discharge SW speed, D (km) is distance between detectors No. 2 and 3, t_a (minutes) is the time needed for the queuing SW to move from the downstream detector to upstream detector, and t_d (minutes) is the time needed for the discharge SW to move from the downstream detector to upstream detector.

Seventeen samples of incidents were used to estimate the queuing and the discharge SW speeds. Figure 2 shows a scatter plot of queuing SW speeds against the arrival rate of vehicles (volume of traffic) and shows

that queuing SW speed is linearly related with the arrival rate of vehicles.

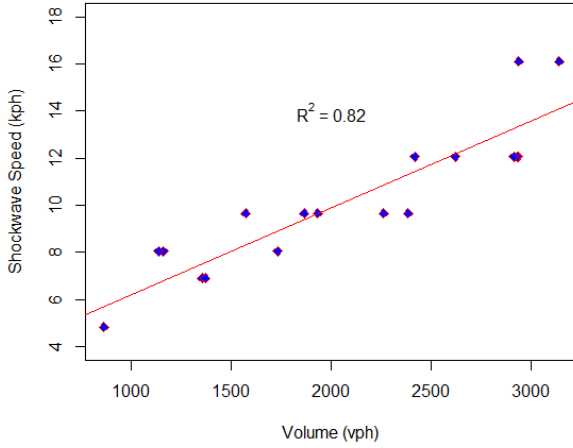


Figure 2 The relation between arrival rate and queuing SW speed as observed from the field

Linear regression was fitted to the scatter plot with an adjusted R-square of 0.82. The arrival rate and queuing SW were related as shown in Equation (3).

$$\text{Queuing SW speed} = 0.0037 \times \text{Arrival rate} + 2.53 \quad (3)$$

As expected, the discharge SW speed was found to be fairly constant regardless of the volume of traffic. This is true because the arrival rate has nothing to do with the speed of vehicles leaving the queue, once the incident blocking the road is cleared. The mean discharge SW speed was estimated to be 17.21 kph.

3.3 Estimating queue length using LWR model

In this section, the general LWR SW model was formulated. Figure 3 exhibits an incidents SW profile of a road segment. Point A is the time and space coordinate that represents the start time and location of an incident. Point B denotes the incident clearing time. Point C shows the time and space coordinate of the last vehicle to join the queue. Point D represents the end of delay generated by the incident from the last vehicle in queue towards the incident location.

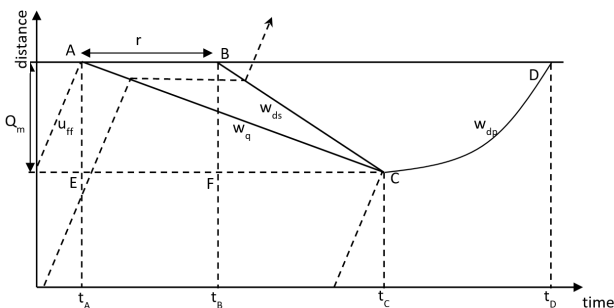


Figure 3 SW profile due to an incident

Let us assume r signifies the incident duration. As indicated in Figure 3, $r = t_B - t_A$, while $t_C - t_B$ defines the total time from the clearing time, i.e. at the moment when the closed lane is opened to traffic, to the moment when the last vehicle joining the queue, $t_D - t_B$ is the total time from the clearing time back to normal condition, i.e. when there were no more delays due to the incident, and Q_m is the maximum queue length. The total delay (TD) is the sum of the areas of $\triangle ABC$ and $\triangle BDC$ multiplied by the density of each associated traffic state.

Given the queuing SW speed w_q and discharge SW speed w_{ds} from Equations (1) and (2), respectively, and the incident duration r , using $\triangle ACE$ and $\triangle BCF$ from Figure 3, the SW speeds can be calculated as in Equations (4) and (5) as follows:

$$w_{ds} = \frac{Q_m}{t_C - t_B} \quad (4)$$

$$w_q = \frac{Q_m}{r + (t_C - t_B)} \quad (5)$$

Equating the Q_m in Equations (4) and (5), the total time from clearing time to the moment the last vehicle enters the queue, $t_C - t_B$ (minutes) can be formulated as shown by Equation (6):

$$t_C - t_B = \frac{w_q \cdot r}{w_{ds} - w_q} \quad (6)$$

Therefore, the queue length Q_m is given by:

$$Q_m = w_{ds} \cdot t_C - t_B \quad (7)$$

The queue length (km) is obtained as in Equation (8) by substituting $t_C - t_B$ in the Equation (6) into Equation (7), expressed as follows:

$$Q_m = \frac{r}{60} \frac{|w_{ds}| \cdot |w_q|}{|w_{ds}| - |w_q|} \quad (8)$$

4 Case Study

4.1 Incident scenario

As discussed in Section 3.2, only incident scenarios which closed both lanes of the HRBT corridor are considered. In this research, an incident scenario was established under moderately congested traffic states with the volume-to-capacity ratio (VCR) of 0.7, or level of service (LOS) C. This traffic condition was selected since it is the states between heavily congested and non-congested traffic conditions. The scenario was implemented for various incident durations ranging from 5 to 40 minutes with 5 minutes increments.

4.2 Calibration of the microsimulation model in VISSIM

HRBT corridor, shown in Figure 1, was coded, calibrated, and validated in VISSIM microscopic traffic simulation software. Observed quantities from the three detectors were used in calibrating the simulation model. As a rule of thumb, the data employed on model validation should be unrelated to the data used for model calibration. Since this study aims to set up a methodology for incident simulation model in VISSIM, the incident-induced queue lengths (obtained from Equation (8)) were utilized to validate the model. Model calibration and validation are iterative processes and continue until the difference between the simulated and observed measures of effectiveness reach an acceptable value.

VISSIM employed ten parameters of car-following driver behavior that can be fine-tuned. These parameters were named CC0-CC9. The first four parameters (CC0-CC3) deal with distance separation between the leading and following vehicles, the subsequent three parameters (CC4-CC6) deal with the speed difference between the leading and following vehicles and the last three parameters (CC7-CC9) deal with acceleration of the following vehicle. For more discussion on VISSIM driver behavior parameters, the reader is referred to [23]. In this study, parameters calibrated to meet the measures of effectiveness are CC0, CC1, and CC2. Brief descriptions of CC0, CC1, and CC2 are as follows:

- CC0 (Standstill distance) is the preferred space between two stationary vehicles. This parameter critically affects the queue length, e.g., queue as a result of lane or road blockage.
- CC1 (Headway Time) is the gap between consecutive vehicles in seconds. This parameter affects the road capacity significantly.
- CC2 (Following Variation) is the extra space beyond safety distance (which is CC0 plus speed of vehicle times CC1) that a vehicle requires and controls the longitudinal oscillation. It influences the capacity of roadways and safety of simulated vehicles.

A modified chi-square statistic (see Equation (9)) GEH (an abbreviation of its inventor name, Geoffrey E. Heavers), was employed to assess the goodness of the calibration process. GEH is advantageous as it considers both the relative and absolute differences between the simulated and observed datasets [24].

$$GEH = \sqrt{\frac{(simulated - observed)^2}{0.5 * (simulated + observed)}} \quad (9)$$

GEH value less than 5 indicates a good fit between simulated and observed measurements, a GEH value in the range of 5 to 10 needs further investigation while a model with a GEH value greater than 10 is assumed to be a bad fit [24].

4.3 Modeling incidents in VISSIM

There are several ways of modeling an incident in VISSIM, and the two most popular are by using a parked vehicle and by using a signal. In this study, a signal-controlled is utilized to mimic the incident as the timing of the signal can be set to represent the incident duration. In this study, a signal-controlled is utilized to mimic the incident as the timing of the signal can be set to represent the incident duration. The signals were installed at the same location of both lanes as in the incident scenario. The traffic signal type operated is a fixed time single-control in the order of red and green signals. To determine the incident-induced queue length in VISSIM, 'queue counters' were used. This feature of VISSIM measures the queue length (in meters) upstream from the site of the incident.

5 Results and Discussion

A microscopic model must be calibrated so that it can replicate the actual traffic conditions. During the initial stage of the calibration process, the length of vehicles standing in the queue generated in the VISSIM model was found to be longer than what is obtained from LWR SW theory. Thus, CC0 value was set to be 5.6 meters to match the queue length suggested by the LWR model. Subsequently, to replicate the actual operation of afternoon freeway traffic (2:00 PM to 4:00 PM) the CC1 and CC2 values were adjusted to be 1.5 sec and 7.5 m, respectively. The average GEH values for traffic counts corresponding to the three detectors are 1.175, 0.989, and 0.828, while for traffic speeds are 2.104, 1.299, and 0.173. The model GEH values for traffic count and traffic speed were 0.997 and 1.192, with standard deviations of 0.711 and 1.150, respectively. For the IPS sensor experiment, one mobile beacon was installed on the moving train while four stationary beacons were installed at the four corners of the miniature's platform. As the train moves on the track, the MINS was used to estimate the train position and the obtained result is plotted against the actual train position in Figure 3. It can be seen in this figure that the IPS estimates closely aligns the actual track of the miniature.

The queue lengths from the VISSIM model and the LWR models were matched for the incident durations

ranging from 5 to 40 minutes by altering the value of the standing distance parameter (CC0). The alteration in the absolute percentage difference between the VISSIM model and LWR model queue length is presented in Figure 4.

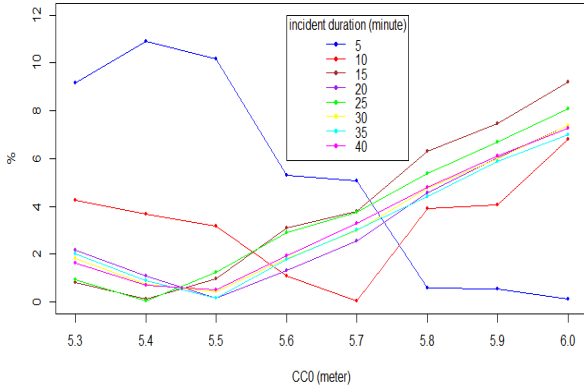


Figure 4 The absolute percentage difference between queue lengths from the LWR model and VISSIM model

Using the average value of the absolute percentage differences in the figure, the best value for CC0 was obtained to be 5.4 m. The model was checked once again for any deviations within the speed and volume from the simulation, and the result showed that there were no significant changes.

The simulation for each incident duration was run 10 times. Since VISSIM produce a stochastic output, the queue length resulted from each simulation is slightly different. The simulation estimated queue length was obtained by taking the average of all simulation queue length. The queue lengths' standard deviation was employed to calculate the upper and lower bounds of the 95% confidence interval (CI), as indicated in Equations (10) and (11).

$$\text{Upper CI bound} = \bar{x} + t_{\frac{\alpha}{2}} \frac{\sigma}{\sqrt{n}} \tag{10}$$

$$\text{Lower CI bound} = \bar{x} - t_{\frac{\alpha}{2}} \frac{\sigma}{\sqrt{n}} \tag{11}$$

Table 1 The result of LWR model and simulation model

| r (minute) | Q _{max-LWR} (km) | Q _{max-VISSIM} | Standard Deviation | Upper bound | Lower bound | Q _{max-LWR} between CI bounds of Q _{max-VISSIM} |
|------------|---------------------------|-------------------------|--------------------|-------------|-------------|---|
| 5 | 2.59 | 2.33 | 0.40 | 2.61 | 2.04 | YES |
| 10 | 5.18 | 5.01 | 0.78 | 5.57 | 4.46 | YES |
| 15 | 7.77 | 7.84 | 0.60 | 8.27 | 7.41 | YES |
| 20 | 10.35 | 10.34 | 0.58 | 10.75 | 9.92 | YES |
| 25 | 12.94 | 13.11 | 0.44 | 13.42 | 12.79 | YES |
| 30 | 15.53 | 15.60 | 0.43 | 15.91 | 15.29 | YES |
| 35 | 18.12 | 18.15 | 0.58 | 18.56 | 17.73 | YES |
| 40 | 20.71 | 20.81 | 0.88 | 21.44 | 20.18 | YES |

Where \bar{x} is the average value of queue length from VISSIM model, σ is the standard deviation, α is the significance level (1 - confidence level), $t_{\frac{\alpha}{2}}$ is the corresponding t value of $\frac{\alpha}{2}$ and n is the number of simulation runs.

Table 1 compares the queue length from the LWR model and VISSIM models. The results confirm that the queue lengths from the LWR model are within 95% confidence interval of the queue lengths from the simulation model. This demonstrates that the incident model in VISSIM is replicating the SW propagations as in LWR model. Figure 5 shows a regression line of the queue lengths versus the incident duration, where the queue lengths increase as the incident durations escalate. The figure also shows the upper and lower bounds of the confidence interval.

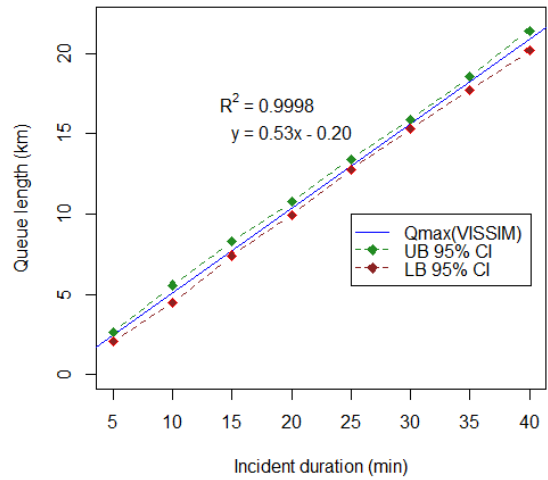


Figure 5 Increase rate of queue length

The results implied that when incidents occur at traffic flow of 1155 veh/h/lane (i.e., VCR of 0.7 or LOS C) the queue length propagate because of incidents blocking both lanes of the freeway is 0.53 km for each minute increment in incident duration.

Equation (12) shows the relationship between queue length (km) and incident duration (minutes).

$$\text{Queue length} = 0.53 \times (\text{Incident duration}) - 0.20 \quad (12)$$

Juxtaposing the approach and the results of this study with other studies are quite challenging, since most incident modeling studies utilizing microscopic traffic simulation directed only on controlled freeway lane closure, for example, work zones [25]. Another study by [26] aimed at simulating incidents-induced capacity reduction but did not investigate the SW speeds and queue length due to the incident.

6 Summary and Conclusion

Freeway operations are negatively affected by several factors, and considerable research effort has been made to address the issues. This study presented a methodology for calibrating incident models in an environment of microscopic traffic simulation. Furthermore, this study has demonstrated that the LWR model constructed using field data can be a proper instrument to calibrate an incident model accurately. The results show that the queue lengths in incident simulation models can be correctly projected for a given incident duration. Such models are useful for apprehending the incidents' impact on freeways and analyzing traffic management strategies to lessen the effect of such random and undesired events.

This study has demonstrated how to obtain more reliable SW speeds using empirical data from freeways and overcome the limitations and bias of the ones obtained from FD. By estimating the SW speeds from the field, this study has confirmed that there is a convincing and linear correlation between the queuing SW speed and arrival rate. On the other hand, this study also has ratified that the discharge SW speed is independent of the vehicle arrival rate. Moreover, the study showed that the results obtained from the field observed SW speeds and LWR model could be used to calibrate an incident model in microscopic traffic simulation model. This can be useful to estimate the benefits of advanced traffic management strategies to minimize the impact of incidents on freeway traffic.

The limitation of this research is that it only considered incidents that cause all lanes to be closed and left out the ones that partially close the freeway. Moreover, since the LWR model is used to obtain queue length, the research suffers from limitations of LWR model as it cannot explain some traffic phenomena, e.g., the stop-and-go traffic conditions and heterogeneous traffic composition [27]. Therefore, future works on this topic will focus on modeling incidents that partially close

freeways and calibrating VISSIM model using queue lengths obtained from the field.

Acknowledgment

The authors would like to thank TranLIVE University Transportation Center, Transportation Research Institute of Old Dominion University (TRI, ODU) and Virginia Department of Transportation (VDOT) for their support to this study.

References

- [1] H. C. Manual, *Highway capacity manual*. Washington D.C.: Transportation Research Board National Research, 2000.
- [2] T. Toledo, M. E. Ben-Akiva, D. Darda, M. Jha, and H. N. Koutsopoulos, "Calibration of microscopic traffic simulation models with aggregate data," *Transportation Research Record*, vol. 1876, no. 1, pp. 10–19, 2004.
- [3] E. Brockfeld, R. D. Kühne, and P. Wagner, "Calibration and validation of microscopic models of traffic flow," *Transportation Research Record*, vol. 1934, no. 1, pp. 179–187, 2005.
- [4] S. Hoogendoorn and R. Hoogendoorn, "Calibration of microscopic traffic-flow models using multiple data sources," *Philosophical Transactions of the Royal Society A: Mathematical, Physical and Engineering Sciences*, vol. 368, no. 1928, pp. 4497–4517, 2010.
- [5] M. J. Lighthill and G. B. Whitham, "On kinematic waves II. A theory of traffic flow on long crowded roads," *Proceedings of the Royal Society of London. Series A. Mathematical and Physical Sciences*, vol. 229, no. 1178, pp. 317–345, 1955.
- [6] P. I. Richards, "Shock waves on the highway," *Operations research*, vol. 4, no. 1, pp. 42–51, 1956.
- [7] J. Li, Q.-Y. Chen, H. Wang, and D. Ni, "Analysis of LWR model with fundamental diagram subject to uncertainties," *Transportmetrica*, vol. 8, no. 6, pp. 387–405, 2012.
- [8] W.-L. Jin, Q.-J. Gan, and V. V. Gayah, "A kinematic wave approach to traffic statics and dynamics in a double-ring network," *Transportation Research Part B: Methodological*, vol. 57, pp. 114–131, 2013.
- [9] X. Wu and H. X. Liu, "A shockwave profile model for traffic flow on congested urban arterials," *Transportation Research Part B: Methodological*, vol. 45, no. 10, pp. 1768–1786, 2011.
- [10] X.-Y. Lu and A. Skabardonis, "Freeway traffic shockwave analysis: exploring the NGSIM trajectory data," in *86th Annual Meeting of the Transportation Research Board, Washington, DC*, 2007.
- [11] S. C. Wirasinghe, "Determination of traffic delays from shock-wave analysis," *Transportation Research*, vol. 12, no. 5, pp. 343–348, 1978.
- [12] H. Mongeot and J.-B. Lesort, "Analytical expressions of incident-induced flow dynamics perturbations: using macroscopic theory and extension of Lighthill-Whitham theory," *Transportation research record*, vol. 1710, no. 1, pp. 58–68, 2000.
- [13] H. Al-Deek, A. Garib, and A. E. Radwan, "New method for estimating freeway incident congestion," *Transportation Research Record*, pp. 30–39, 1995.
- [14] R. D. Kuhne, "Foundations of Traffic Flow Theory I: Greenshields' Legacy—Highway Traffic," in *Symposium on the Fundamental Diagram: 75 Years (Greenshields 75 Symposium) Transportation Research Board*, 2008.

- [15] B. D. Greenshields, W. Channing, and H. Miller, "A study of traffic capacity," in *Highway research board proceedings*, 1935, vol. 1935.
- [16] S. L. Dhingra and I. Gull, "Traffic flow theory historical research perspectives," *The fundamental diagram for traffic flow theory*, p. 45, 2011.
- [17] D. Ngoduy, "Multiclass first-order traffic model using stochastic fundamental diagrams," *Transportmetrica*, vol. 7, no. 2, pp. 111–125, 2011.
- [18] B. S. Kerner, "Three-phase traffic theory and highway capacity," *Physica A: Statistical Mechanics and its Applications*, vol. 333, pp. 379–440, 2004.
- [19] F. L. Hall, "Traffic stream characteristics," *Traffic Flow Theory. US Federal Highway Administration*, vol. 36, 1996.
- [20] L. Chu, H. X. Liu, J.-S. Oh, and W. Recker, "A calibration procedure for microscopic traffic simulation," in *Proceedings of the 2003 IEEE International Conference on Intelligent Transportation Systems*, 2003, vol. 2, pp. 1574–1579.
- [21] B. Park, J. Won, and I. Yun, "Application of microscopic simulation model calibration and validation procedure: Case study of coordinated actuated signal system," *Transportation Research Record*, vol. 1978, no. 1, pp. 113–122, 2006.
- [22] A. Kesting and M. Treiber, "Calibrating car-following models by using trajectory data: Methodological study," *Transportation Research Record*, vol. 2088, no. 1, pp. 148–156, 2008.
- [23] P. T. V. Vision, "VISSIM 5.30-05 User Manual," *Planung Transport Verkehr AG: Braunschweig, Germany*, 2011.
- [24] P. Holm, D. Tomich, J. Sloboden, and C. Lowrance, "Traffic Analysis Toolbox Volume IV: Guidelines for Applying CORSIM Microsimulation Modeling Software," Jan. 2007.
- [25] Z. Zhu, "Calibration of Work Zone Impact Analysis Software for Missouri," 2013.
- [26] M. Hadi, P. Sinha, and A. Wang, "Modeling reductions in freeway capacity due to incidents in microscopic simulation models," *Transportation Research Record*, vol. 1999, no. 1, pp. 62–68, 2007.
- [27] S. Logghe and L. H. Immers, "Multi-class kinematic wave theory of traffic flow," *Transportation Research Part B: Methodological*, vol. 42, no. 6, pp. 523–541, 2008.